JOURNAL OF MATERIALS SCIENCE 20 (1985) 3439–3452

An electron microscopic study of the morphology of cured epoxy resin

V. B. GUPTA*, L. T. DRZAL, W. W. ADAMS
Materials Laboratory (AFWAL/MLB), Wright-Patterson AFB, Ohio 45433, USA
R. OMLOR
Systems Research Laboratories, Indian Ripple Road, Dayton, Ohio 45440, USA

An electron microscropic study of fracture surfaces and microtomed sections of a cured epoxy resin based on a difunctional bisphenol A type resin cured with different amounts of *m*-phenylenediamine is presented. Heterogeneities in the range 5 to 100 nm are seen to be present and have relatively higher crosslink density compared to the surrounding matrix. It is observed that the fracture path is around the heterogeneity and not through it. The size of the heterogeneity is a function of curing agent concentration and also of cure cycle. The stoichiometric sample, which has the highest crosslink density and the highest glass transition temperature, has the smallest heterogeneities. On either side of stoichiometry, the heterogeneity size increases. Samples subjected to a more severe post-curing cycle have much larger heterogeneities. The possible physical basis for these differences is discussed.

1. Introduction

The morphologies of a number of cured epoxy resin systems have been studied by electron microscopy, and considerable evidence has been obtained or the existence of heterogeneities at the 5 to 100 nm size level [1–11]. These heterogeneities have been shown to be regions of high crosslink density in a matrix of relatively lower crosslink density. However, these studies have also generated a number of controversies. Oberlin *et al.* [1] studied ultramicrotomed 40 nm thick sections of a cured epoxy resin system with the electron microscope column under "clean" vacuum obtained by ionic pumping, and imaged, what they claimed to be, single molecules of the epoxy resin used. At vacuum levels used in the normal microscopes: 10^{-4} to 10^{-5} torr, "nodules" of 10 nm size having a local order higher than that of the bulk became visible. It was therefore concluded that freshly prepared resin is homogeneous and remains stable while under study in a clean vacuum. In poorer vacuum, electron irradiation etches the sample and inhomogeneities develop. Aspbury and Wake [2] studied ultramicrotomed sections of some other epoxy systems which were shadowed with platinum–carbon. They identified the basic nodular feature to be of about 5 nm in size, but found that aggregates of nodules 10 to 40 nm in size were by far the most notable features of the electron micrographs. Studies on the morphology of cured epoxy systems as a function of curing agent concentration have been made using etched surfaces and fracture surfaces or their replicas, and heterogeneties in the 10 to 60 nm size range have been identified; their sizes depended strongly on curing agent concentration [3–7]. However, while Racich and Koutsky [3, 4] and Mijovic and Koutsky [5] concluded that lower stoichiometries had entities of larger size, Mason *et al.* [6] and Misra *et al.* [7] found that higher stoichiometries had larger heterogeneities. Bell [8] and Takahama and Geil [9] have also shown that

*On leave from the Indian Institute of Technology, New Delhi 110016, India.

0022–2461/85 $03.00 + .12

heterogeneities of 10 to 50 nm size exist in cured epoxy resins. Morgan and O'Neal [10] present evidence for 8 to 9 nm sized heterogeneities which aggregate into larger entities. Bell [8] has additionally shown that the degree of mixing of the reactants can affect the homogeneity of the cured resin system, and the size of the heterogeneity would therefore be a function of the degree of mixing.

In addition to electron microscopy, the existence of heterogeneities has also been inferred from studies based on various other techniques [12–15]. Electron paramagnetic resonance (EPR) studies on cured epoxy resin have given evidence [12, 13] for two phases, and it was shown that solvents are preferentially sorbed in the low crosslink regions which have greater free volume content. Nuclear magnetic resonance (NMR) studies of epoxy resins [13] have shown the existence of mobile and rigid regions, and the size of the rigid regions has been found to be in the 22 to 46 nm range. Matyi *et al.* [14] found evidence for inhomogeneities in the size range of 10 to 100 nm, with the most frequent size range being 10 to 20 nm by small-angle X-ray scattering. They stated that heterogeneities could either be regions that differ in crosslink density or gas bubbles. Kreibich and Schmid [15] showed that annealing can cause phase separation of the high and low crosslinked phases, and this results in a splitting of the glass transition temperature. Such an effect could, however, also arise from a transient phase due to ageing [16].

The non-uniformity of crosslink density can have important consequences on the properties of the cured epoxy resin. Therefore there has been considerable interest in studying the origin of the heterogeneities in these systems. But it is still not clear why, when, and how they form. Extremely divergent views have been expressed. Funke [17, 18] states, in a discussion of the reaction mechanisms leading to the formation of crosslinked systems, that the formation of homogeneous networks represents an exception in crosslinking polymerization. A similar conclusion was reached by Labana *et al.* [19]. Lunak and Dusek [20] and Dusek *et al.* [21], on the other hand, have postulated that epoxies are more likely to have a homogeneous structure. Deanin [22] has described how inhomogeneities may form during crosslinking of an initially homogeneous resin. When a reactive polyfunctional low molecular weight monomer reacts with a crosslinking agent, the statistical probability of forming each new bond is equal throughout the material. When the molecular weight has grown to a certain critical size, the molecule is no longer small enough to remain uniformly dispersed in the liquid medium by Brownian motion and begins to segregate out in the form of a rubbery gel. With further reaction within this segregated mass, the amount of available reacting species in the neighbourhood is reduced. The final cured product contains highly crosslinked particles separated by relatively weakly bound interfacial area. Bobalek *et al.*]23], Solomon [24] and Labana *et al.* [19] have suggested that the two-phase system is produced before the formation of the macrogel. Apicella *et al.* have postulated [25] that inhomogeneous networks form during post-curing. Stevens *et al.* [26] investigated local order in unreacted DGEBA epoxy resin monomer by Rayleigh scattering and Brillouin spectroscopy, and showed that aggregates of 20 to 70 nm size were present in the resin and were caused by differences in intermolecular hydrogen bonding, which was related to the epoxide/hydroxyl ratio of the resins. They suggested that this local order in the unreacted resin could promote inhomogeneous reaction and lead to network inhomogeneity. Luttgert and Bonart [27] have postulated that the size of the heterogeneity in the cured resin depends on the rate of microgel formation or nucleation and on the rate of growth of the gel particles. At high curing temperatures, the rate of nucleation will be fast and the great number of microgels formed permits growth only to a small size. Low curing temperaturtes initiate only a small number of gel particles, and the cured resin will show large globular heterogeneities.

In the present investigation, the cured epoxy resin system studied was based on the diglycidyl ether of bisphenol A (DGEBA), which was cured with different amounts of *m*-phenylenediamine (*m*PDA) under two curing cycles. The studies included transmission electron microscopy (TEM), scanning electron microscopy (SEM) and scanning transmission electron microscopy (STEM) of unetched and etched fracture surfaces and their replicas and of unstained and stained microtomed sections. Heterogeneities in the 5 to 100 nm range were

found to be the predominant feature and their size was a function of curing agent concentration and cure history. Broadly speaking, the size was smallest for samples containing the stoichiometric amount of curing agent and increased on either side of stoichiometry. The size of the heterogeneity also showed considerable increase on post-curing. Possible reasons for these are discussed.

2. Experimental procedure

The epoxy resin used was Epon 828 (Shell), which is based on DGEBA and has the following chemical struture:

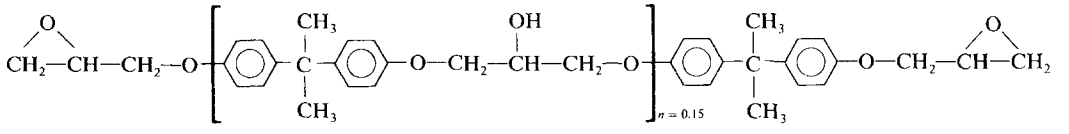

It is a liquid of high viscosity at room temperature with an epoxide equivalent of 190. The curing agent used was *m*-phenylenediamine (*m*PDA), an aromatic amine that is a solid at room temperature with a melting point of 68° C. It has the following chemcial structure:

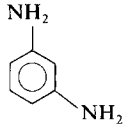

The epoxy molecule has two epoxy groups while the curing agent has four active hydrogens. For all the epoxide groups to react, 14.5 parts by weight of *m*PDA per 100 parts by weight of Epon 828 are required; this is the stoichiometric amount of curing agent. In the present investigation, the resin was cured with 7.5, 10, 14.5, 20 and 25 phr of curing agent.

The resin and the curing agent were heated in separate containers in an oven set at 75° C. When the *m*PDA had melted completely, it was mixed with the epoxy resin and then degassed under vacuum for 7 min. Degassing removes the air bubbles and at the same time vigorous mixing takes place. The mixture was then cast into rectangular bars, dogbone coupons, and thin discs by pouring into flexible silicone rubber moulds which were open at the top. The curing cycle used was 2 h at 75° C followed by 2 h at 125° C. The oven was then switched off and the cured samples allowed to cool within the oven until they reached room temperature; this took about 4 h. These samples will be designated as "standard cure". Another set of samples was prepared by post-curing the standard cure samples at 175° C for 6 h in an inert-gast environment; they will be referred to as the "post-cured" samples. While detailed studies were conducted on the standard cure samples, only a limited amount of work was done on the post-cured samples.

A notch was made on the narrowest side of the rectangular specimen with a rotating cutter and the crack so formed was gently touched under slight pressure with a fresh razor blade. The two ends of the sample were held with pliers and immersed in liqid nitrogen. The sample was taken out from the liquid nitrogen bath after some time and then immediately fractured by bending around the notch. Some of the fracture surfaces were etched for 30 min in an argon plasma using 50 W power at about 20 ml min^{-1} flow of argon gas and 0.5 mm mercury pressure using an International Plasma Corporation unit. The temperature inside the plasma unit was measured with a thermocouple and after 30 min was found to be 65° C. The as-fractured and plasma-etched fracture surfaces were coated with gold–palladium on a sputtering unit, and the coated surfaces were examined on an ETEC Autoscan scanning electron microscope and on the Jeol scanning transmission electron microscope in the scanning mode.

It has been shown [28] that the usual method of preparing replicas of epoxy surfaces, i.e. the use of polyacrylic acid as the replicating fluid, can give rise to artifacts. Hence a modified replication technique was developed and used [29]. The replicas were examined on a Jeol 100CX scanning transmission electron microscope in the transmission mode.

Some studies were also made on plasma-etched as-cured surfaces of the standard cure samples in the SEM and on their replicas in the TEM.

Microtomed sections were prepared by cutting thin sections of standard cure samples on an Ultracut, Reichert Ultramicrotome using a diamond knife at room temperature. Though the

thickness of the microtomed sections was not measured, it was expected to be in the 50 nm range. Some of the sections were mounted on unsupported fine nickel grids, stained in 10% osmium tetroxide in benzene and allowed to dry at room temperature. Some dilute solution infrared analysis was conducted to determine the location of osmium tetroxide reaction. Results from this study showed that primary and secondary amines were attacked by osmium tetroxide but that tertiary amines were not. It was therefore suspected that incompletely reacted amine sites, which will be present in relatively greater quantity in the low crosslink density matrix phase, will be preferentially stained. The stained sections were examined on an optical microscope, and they showed quite uniform staining; the samples with excess amine were relatively darker. The stained sections were then examined on the SEM and STEM. An energy-dispersive X-ray scan of this sample for osmium was made.

3. Results and discussion

From the initial exploratory work, it was quite clear at the outset that the fracture surfaces of cured epoxy resin samples contained inhomogeneities in the 5 to 100 nm range. The relative merits of the various techniques of sample preparation were therefore evaluated in relation to the clarity with which they revealed the underlying structure in a reproducible manner. The samples included as-cured surfaces etched for 90 min in cold argon plasma, unetched and 30 min plasma-etched fracture surfaces, and unstained and stained microtomed sections with uranyl acetate and osmium tetroxide as the staining agents. While all these techniques revealed the presence of heterogeneities, the plasma-etched fracture surfaces and the osmium tetroxide stained ultramicrotomed sections gave the most satisfactory and reproducible results. Among the examination techniques, use was made of SEM, TEM, and STEM.

3.1. Plasma-etched fracture surfaces

The fracture surfaces of the standard cure samples etched with a cold argon plasma for 30 min were first examined on the ETEC Autoscan scanning electron microscope. The scanning micrographs of the fracture surfaces of samples with the five stoichiometries are shown in Figs. 1a to e. The heterogeneous morphology is distinctly visible, and there are differences in the size and size distribution of the heterogeneities in the five samples. From enlarged photographs, the sizes of about 200 entities were measured; in all cases they were found to fit a log normal distribution and are shown in Fig. 2 as linear plots of size on log-probability paper. The median value at 50% cumulative frequency was taken as the average size of the heterogeneity. The variation of the average size with curing agent concentration is shown in Fig. 3. The stoichiometric sample, which has the maximum crosslink density and the maximum T_g [30], has the smallest heterogeneity. On either side of stoichiometry, the heterogeneity size increases as crosslink density and T_g decrease.

The plasma-etched fracture surfaces of the post-cured samples were next studied on the Jeol 100CX STEM in the scanning mode. The scanning micrographs for the five stoichiometries are shown in Figs. 4a to e. Distinct heterogeneous morphology is seen and the heterogeneities are now larger is size. No detailed size distribution studies were made on these micrographs, but it appeared that in these samples the sizes were larger by a factor of about 2 to 3 relative to the standard cure samples. Also the stoichiometric samples still had the smallest size heterogeneity. Possible reasons for this increase in heterogeneity size on post-curing will be discussed later.

Dusek *et al.* [21] studied the fracture surfaces of two amorphous thermoplastic polymers, i.e. polystyrene and polymethyl methacrylate, along with those of cured epoxy resin by electron microscopy. They used an air plasma to etch the fracture surface and observed inhomogeneities of 20 to 40 nm size in all the samples. Since amorphous polystyrene and polymethylmethacrylate (PMMA) are believed to be homogeneous, the authors concluded that the inhomogeneous structure is not an inherent property of the cured epoxy resins and apparently the effects that are seen are artifacts resulting from plasma etching. It was therefore considered worthwhile to study the fracture surfaces of these amorphous thermoplastics when etched with an argon plasma. A thin sheet of atactic polystyrene was melt-pressed from polystyrene of molecular weight 200 000 and M_w/M_n close to unity (supplied by Pressure Chemical Co,

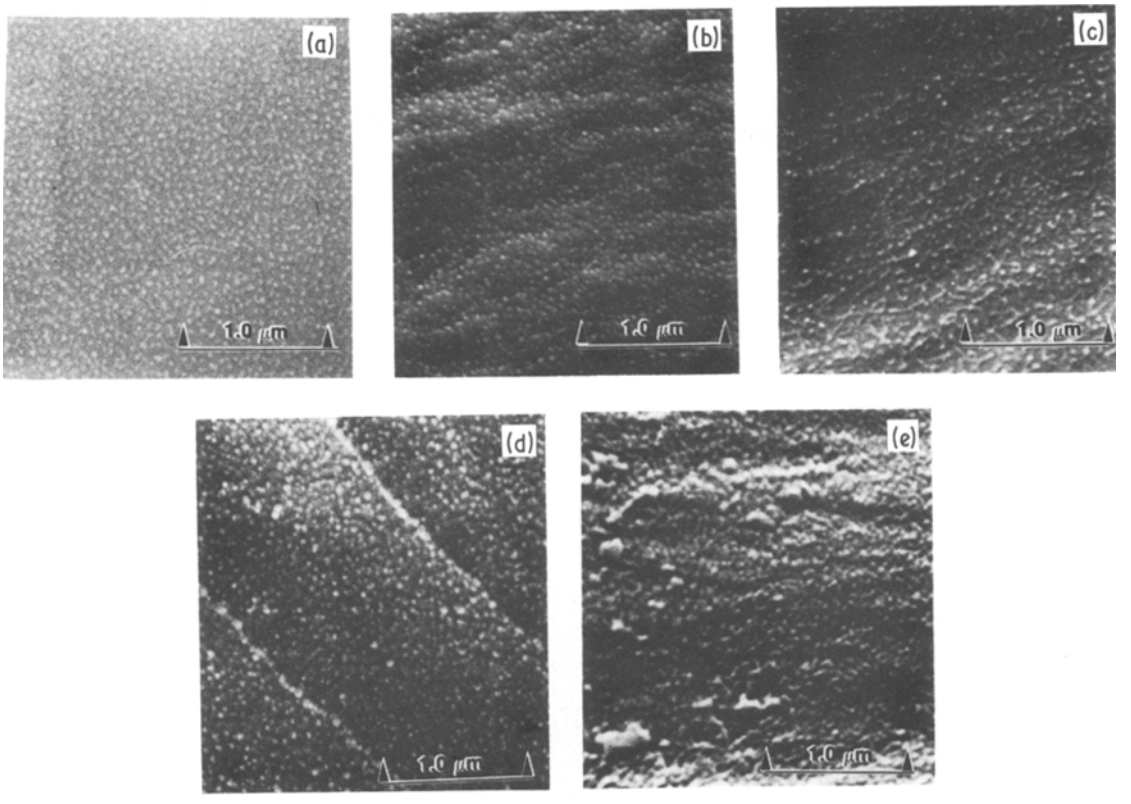

Figure 1 Scanning electron micrographs of plasma-etched fracture surfaces of standard-cure samples: (a) 7.5 phr, (b) 10 phr, (c) 14.5 phr, (d) 20 phr, (e) 25 phr.

Pittsburgh, Pennsylvania, USA). This and a commercial "Plexiglas" sheet (Rohm and Haas, USA) were then fractured in liquid nitrogen and etched with argon plasma under the same conditions as used for the epoxy specimen. As shown in Figs. 5a, b and c, the low-magnification scanning micrographs of the fracture surfaces indicate that there is extensive plastic deformation in the amorphous thermoplastics but not in the epoxy sample. At higher magnification, the amorphous thermoplastics are relatively featureless as shown in Figs. 5c and d, but the epoxy sample (Fig. 5e) shows heterogeneities in the 5 to 50 nm range. Thus the heterogeneities in the plasma-etched epoxy fracture surfaces may not be an artifact. The experiments of Dusek *et al.* [21] differed from those reported here in two respects: first, they used an air and not an argon plasma; and secondly, they studied a replica of the fracture surface using polyvinyl alcohol in water as the replicating agent and not the fracture surface itself. It would be interesting

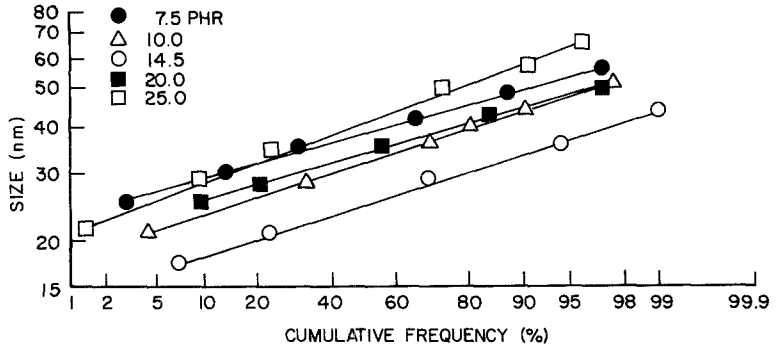

Figure 2 Size distribution of heterogeneities of the standard-cure samples containing different amounts of curing agent.

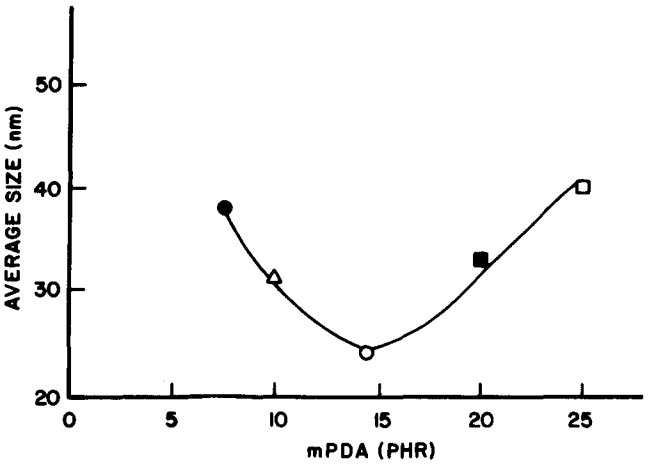

Figure 3 Variation of the average size of the heterogeneities of the standard-cure samples with curing agent concentration (symbols as Fig. 2).

to find out if these factors resulted in introducing the artifacts.

The existence of heterogeneous morphology in all the samples was confirmed by using a modified replication technique [29], which involved the coating of the fracture surface with in thin film of carbon before replicating it. As an illustration, the transmission micrograph of the replica of the 30 min plasma-etched fracture surface of the stoichiometric sample is shown in Fig. 6 along with the scanning micrograph of the fracture surface at a similar magnification

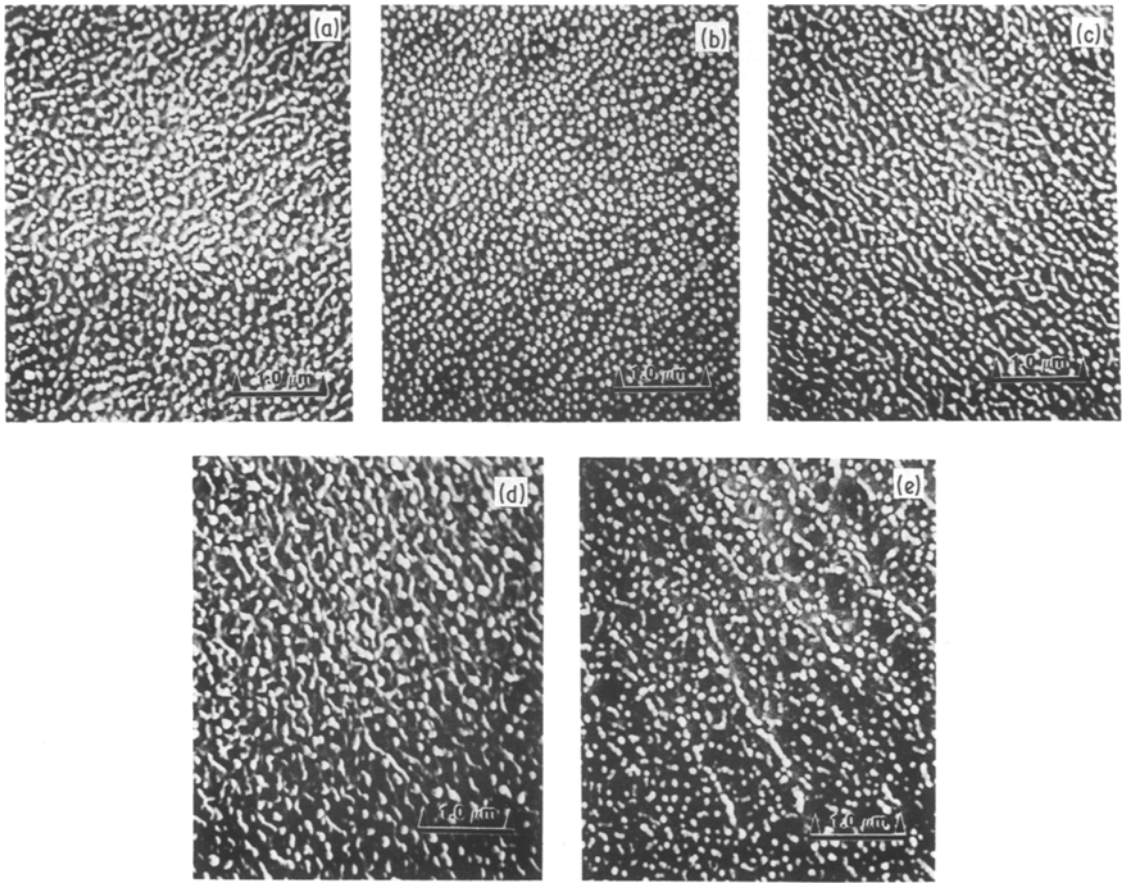

Figure 4 Scanning micrographs of plasma-etched fracture surfaces of post-cured samples: (a) 7.5 phr, (b) 10 phr, (c) 14.5 phr, (d) 20 phr, (e) 25 phr.

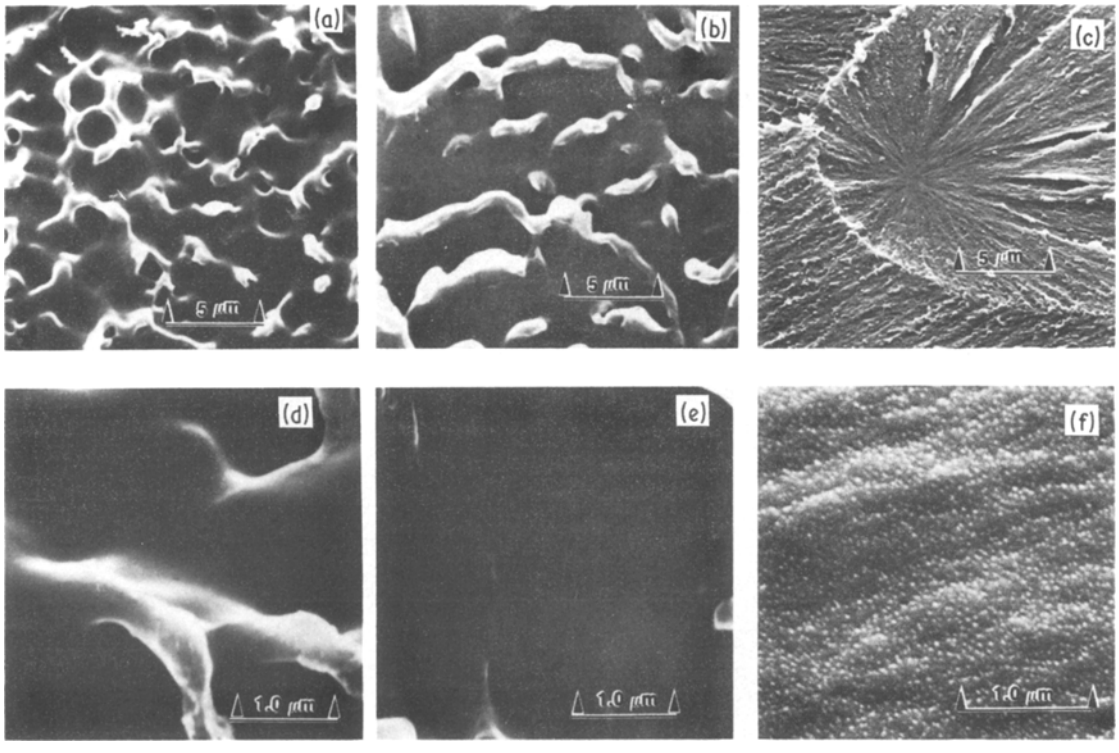

Figure 5 Scanning micrographs of plasma-etched fracture surfaces. At low magnification: (a) PMMA, (b) atactic polystyrene, (c) standard-cure epoxy resin with 10 phr *m*PDA. At high magnification: (d) PMMA, (e) atactic polystyrene, and (f) standard-cure epoxy resin with 10 phr *m*PDA.

for comparison. The heterogeneities are quite well resolved in the replica micrograph, and their size distribution and average size are quite close to those obtained from the earlier data.

3.2. Plasma-etched as-cast surfaces

It has been stated that the fracture process itself can introduce the types of features that are being observed: spherical entities in the 5 to 100 nm range [31]. The as-cured surface of the stiochiometric sample plasma-etched for 90 min was therefore studied on the SEM and its replica on the STEM in the transmission mode. As shown in Figs. 7a and b, a network of interconnected inhomogeneities is distinctly seen on the as-cast surface. The size of the heterogeneity is consistent with earlier data obtained from the fracture surfaces. Detailed studies on samples of different stoichiometry showed that the results were not always reproducible. A likely reason for this is that the as-cured surface, which was exposed to air during curing, could lose some amine and thus have a morphology that is not representative of the bulk.

3.3. Microtomed sections

The as-microtomed sections of the standard-cure sample containing stoichiometric amounts of curing agent were examined on the STEM in the transmission mode, and a series of through-focus micrographs were taken. As shown in Fig. 8, which is the in-focus micrograph, heterogeneities in the 5 to 30 nm size range are seen; however, they are not very distinct. The microtomed sections of atactic polystyrene were similarly examined, and the through-focus series of micrographs (Fig. 9) show a rather featureless surface and do not reveal any recognizable morphological entities. The as-microtomed section of the standard-cure sample containing the stoichiometric amount of curing agent was shadowed with carbon–platinum and, as shown in Fig. 10, entities of 5 to 20 nm size can be seen in the surface. Such shadowing did not bring out any structure in atactic polystyrene.

Next, the microtomed sections stained with osmium tetroxide were examined on the STEM in the transmission and scanning transmission modes. As stated earlier infrared studies had

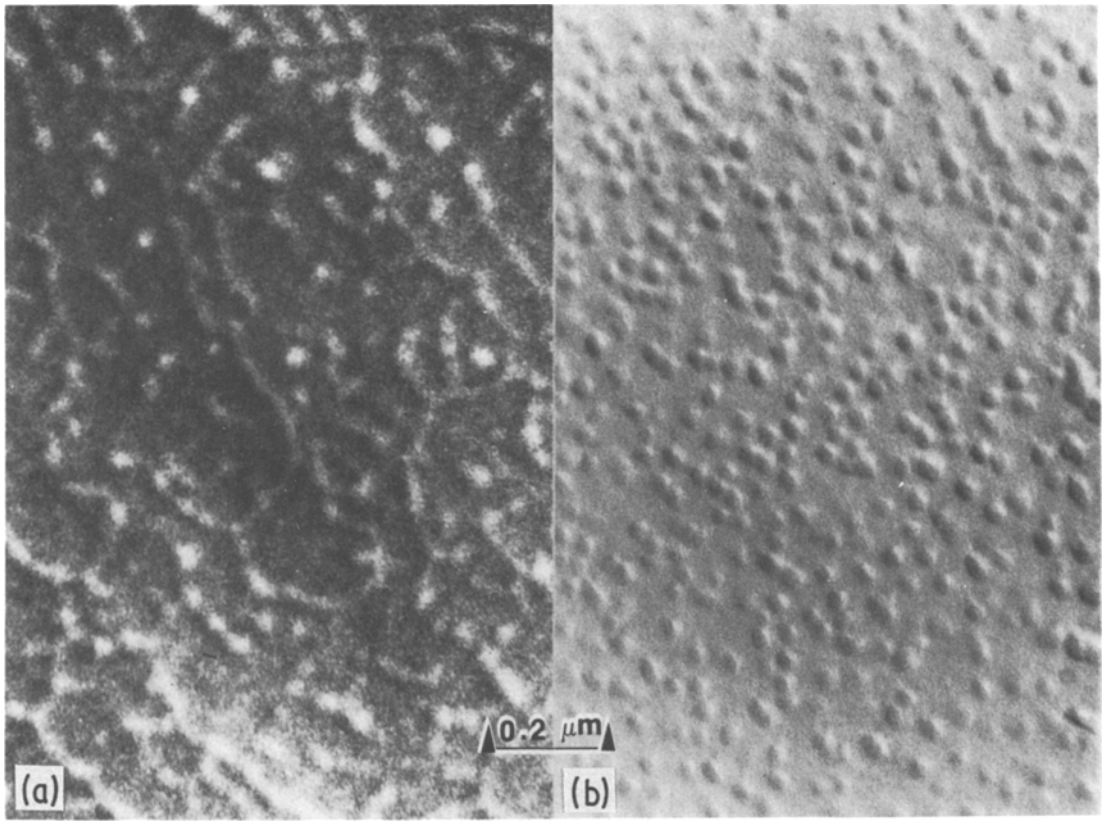

Figure 6 Micrographs of fracture surfaces of plasma- etched standard-cure stoichiometric samples: (a) scanning micrograph, (b) transmission micrograph of replica.

shown that osmium tetroxide attacks the primary and secondary amines. Since there would be more unreacted amine in the less crosslinked regions, it would be expected that the boundaries around the heterogeneities will be stained to a relatively higher degree and thus would appear dark in the micrographs. However, since the thickness of the sections examined is at least twice the heterogeneity size, the entities in the path of the electron beam will overlap and distinct boundaries would not be expected to show up. The micrograph shown in Fig. 11a for the standard cure, 14.5 phr sample shows reasonably distinct boundaries of entities indicated by arrows. To emphasize this effect, a low exposure print of the same micrograph is also included (Fig. 11b) as it defines the boundaries more clearly. The size of the entities is consistent with the earlier data. An energy-dispersive X-ray scan of this sample for osmium showed (Fig. 12) that osmium is non-uniformly distributed in the sample in a manner similar to the distribution observed in the TEM and SEM micrographs. A micrograph of an osmium tetroxide stained sample of different stoichiometry, i.e. 25 phr standard cure sample (Fig. 13), also shows dark stained rings around the heterogeneity.

Some authors have suggested [2, 10] that the heterogeneities in the 20 to 60 nm range are aggregates of basic "nodules" of around 5 or 8 nm size. In the present studies, the osmium tetroxide stained sections, as shown in Figs. 11a and 13, do indicate that the heterogeneities could indeed be aggregates of smaller entities. However, careful and detailed studies are required to verify this since the size of the smaller entities is close to the statistical noise of the microscope. This work is under consideration.

During investigation of a microtomed section of a sample prepared from X-22 resin, which is a purified form of Epon 828, containing stoichiometric amounts of *m*PDA, an interesting result was obtained. When this sample was being

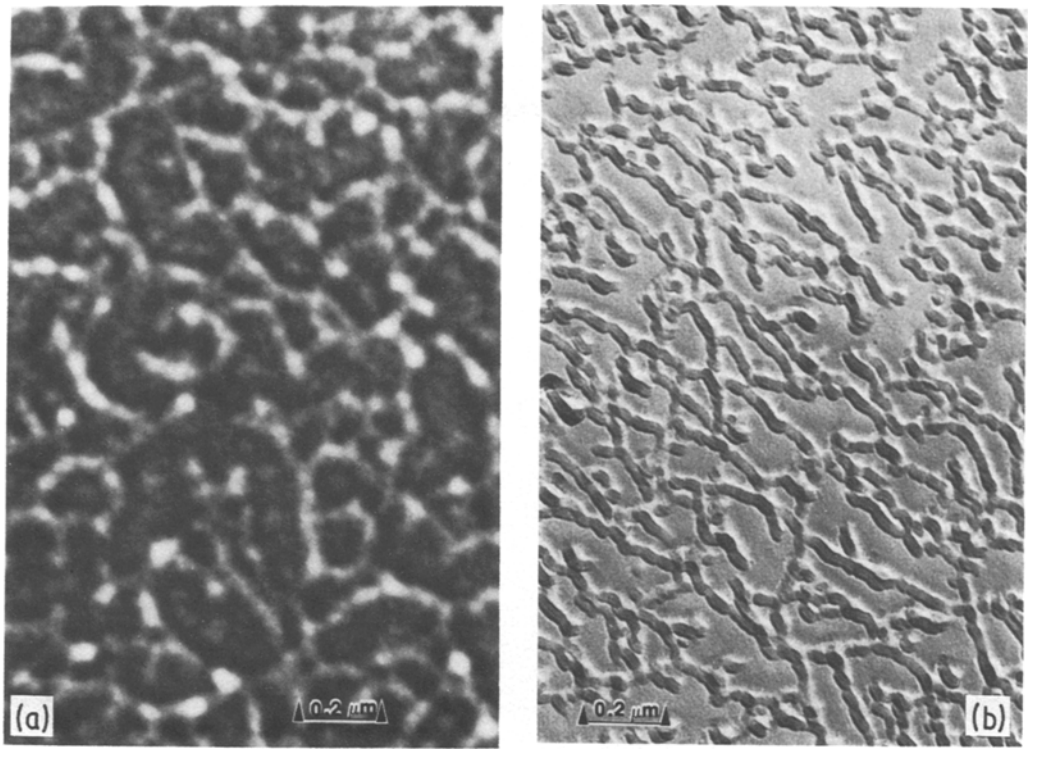

Figure 7 Micrographs of plasma-etched as-cured surface of the standard-cure stoichiometric sample: (a) scanning micrograph, (b) transmission micrograph of replica.

examined on the electron microscope, beam damage caused two holes in the specimen and this resulted in tearing of the film along the arrows indicated in Fig. 14. A 200 nm wide strip can be seen bridging the advancing tears and is apparently under considerable stress. Under this stress the sample appears to have stretched, and since this part of the section has become thin, the heterogeneities and the dark stained rings around them can be seen more distinctly. A dark band, which at its narrowest is around 5 nm wide, runs through the middle of this strip, and it is clear that rupture is more likely to occur along this band. This dark band is apparently formed as a result of the alignment of the heterogeneities and represents the boundary

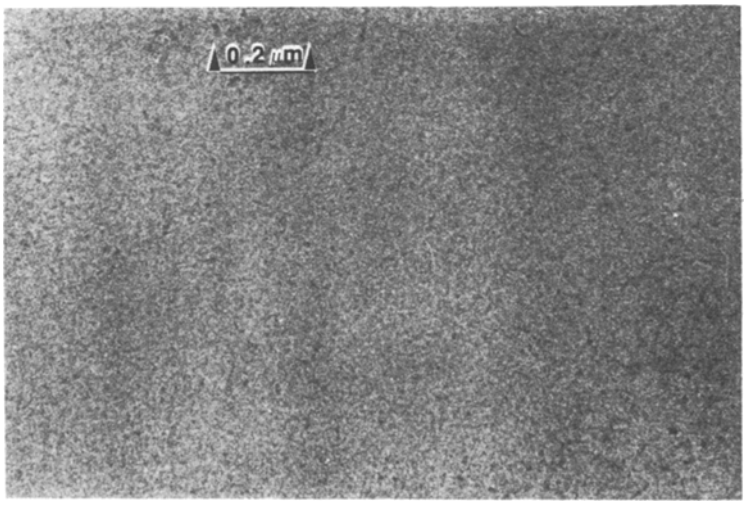

Figure 8 Transmission micrograph of ultramicrotomed section of standard-cure stoichiometric sample.

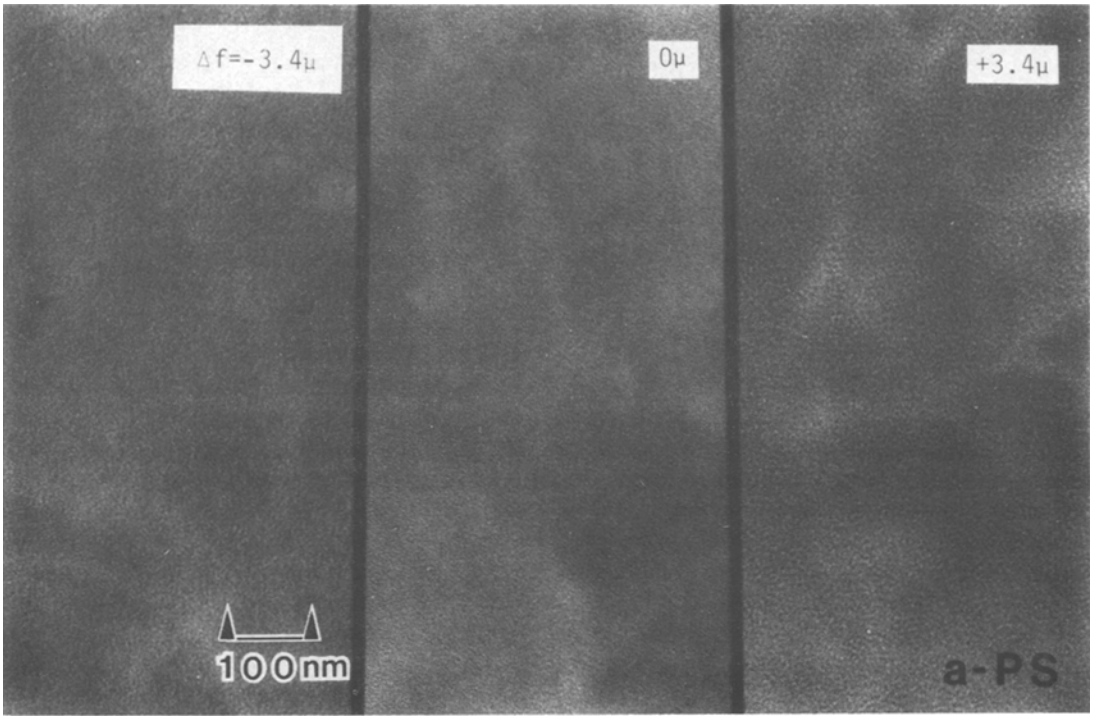

Figure 9 Transmission micrographs of ultramicrotomed section of atactic polystyrene: through-focus series.

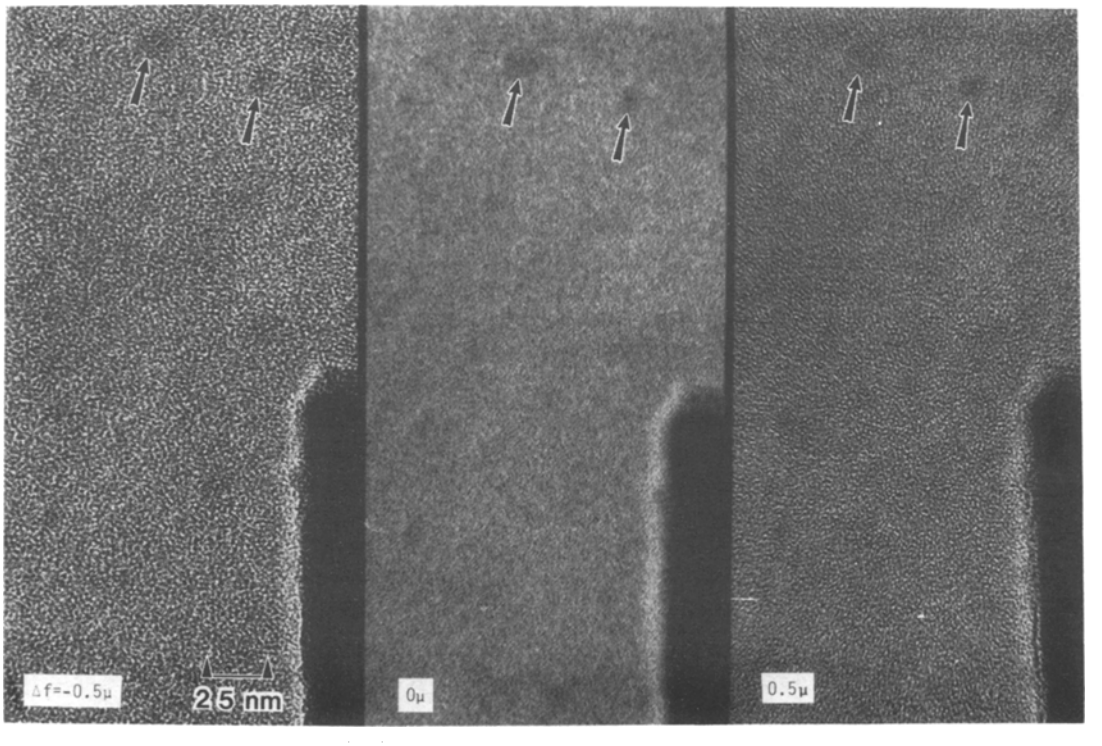

Figure 10 Transmission micrographs of C–Pt shadowed ultramicrotomed section of standard-cure stoichiometric sample: through-focus series.

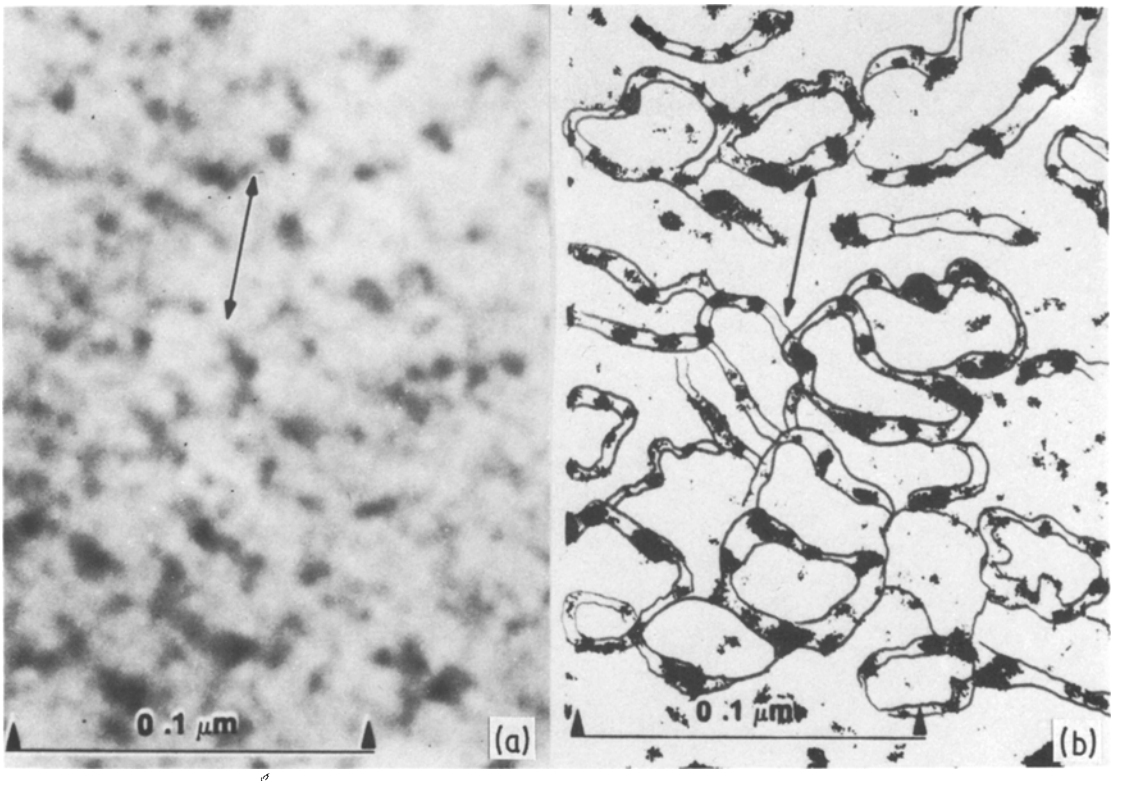

Figure 11 (a) Transmission micrograph of osmium tetroxide stained standard-cure stoichiometric sample, (b) the same micrograph printed with a different exposure time.

between them. Close examination of this micrograph shows that the circular features observed in the normal stained thin sections are now elongated into elliptical shapes. From prints of this micrograph at various exposure times, the heterogeneity boundaries could be traced in a number of cases and, as shown in Fig. 15, follow the stress field by deforming and/or aligning suitably.

4. The heterogeneity size

4.1. The standard cure samples

Data on size distribution and average size of the heterogeneity for the standard cure samples were presented earlier in Figs. 2 and 3. The sample with the stoichiometric amount of curing agent (14.5 phr) has heterogeneities of the smallest size.It has been shown elsewhere [30] that this sample has the highest crosslink density and also the highest glass transition temperature (T_g).

The stoichiometric sample has the right proportion of resin and curing agent so that each epoxy group has an active amine hydrogen to react with in the reacting mass. Assuming that the resin and the curing agent are well mixed, the stoichiometric sample will form a network in which, in the ideal case, all epoxy and amine groups will have reacted. In the other samples there is an excess of either epoxy or amine, and the cured sample will therefore contain unreacted epoxy or amine groups. Infrared studies reported elsewhere [30], broadly speaking, confirm these expectations. In an exothermally reacting mass, the greater the temperature rise, the larger the number of nuclei, as postulated by Luttgert and Bonart [27]. Though some attempts were made to monitor the temperature rise during the curing cycle, a consistent picture did not emerge and no comments will therefore be made on this aspect at this stage. The nuclei so formed will continue to grow till the growing network reaches its T_g. Once the network has reached its T_g, the diffusion of the reacting species will be hindered and the reaction will soon be quenched. The T_g data for the standard cure samples [30] are summarized in Table I. The data for the post-cured samples are also included in this table since they are required at a

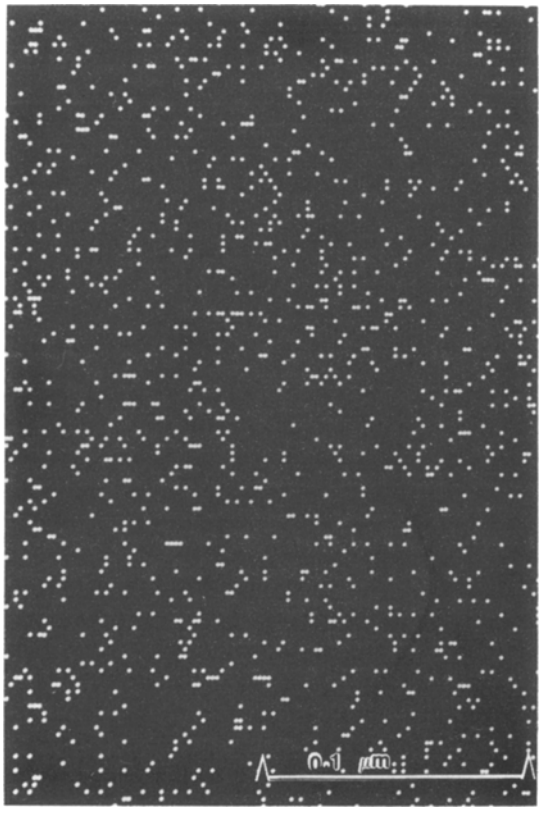

Figure 12 Energy dispersive X-ray scan of the standard-cure stoichiometric sample for osmium.

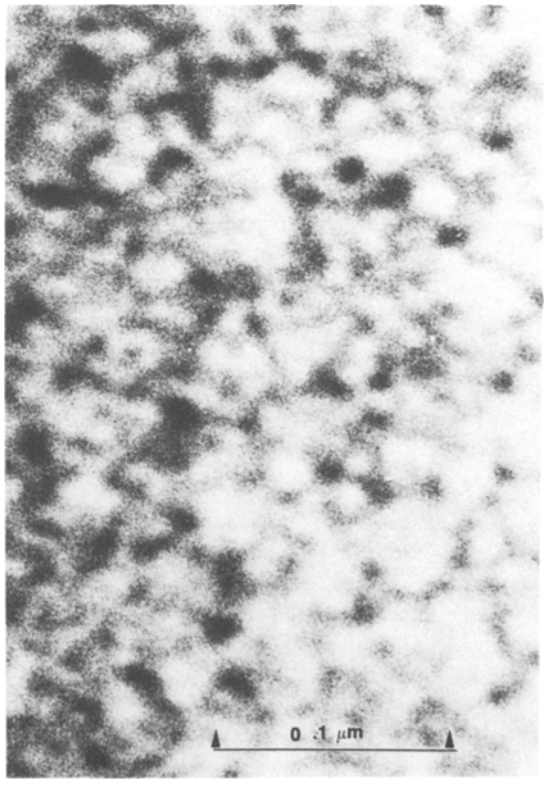

Figure 13 Transmission micrograph of osmium tetroxide stained standard-cure sample containing 25 phr of *m*PDA.

later stage. It is noteworthy that the T_g of the standard cure, stoichiometric sample (145° C) is higher than the final cure temperature (125° C) for this sample. A phenomenological model to explain the heterogeneity size data emerges from this discussion. In the stoichiometric samples, since the reacting mass has the correct proportions of resin and curing agent, network formation is rapid and the approach to a T_g of 145° C is apparently fast. The reaction is quenched at quite an early stage, thus allowing the nuclei to grow only to a small size heterogeneity. In the other samples unreacted groups get incorporated, and the network approaches its T_g rather slowly. Since the T_g values of all these other samples are lower than the final cure temperature, these samples will be in the rubbery state throughout the cure cycle when some form of reaction can continue to take place. The heterogeneities will consequently be larger in size.

TABLE I Glass transition temperature data as obtained from differential scanning calorimetry

Stoichiometry (phr of *m*PDA)	Glass transition temperature (° C)	
	Standard cure	Post-cured
7.5	55	71
10.0	76	134
14.5	145	160
20.0	116	120
25.0	95	102

4.2. The post-cured samples

The effect of post-curing on heterogeneity size has not been extensively studied. Yamini and Young [11] report that when samples cured at room temperature for 24 h were post-cured at 100 and 150° C, the size of the heterogeneity decreses dramatically with increase in the post-curing temperaute. Aspbury and Wake, [2] on the other hand, report that when samples that had first been cured at 60° C for four days were post-cured at 150° C, the heterogeneity size was almost doubled. Our results are similar to those of Aspbury and Wake [2]. For our post-cured samples, the T_g data are given in Table I and it

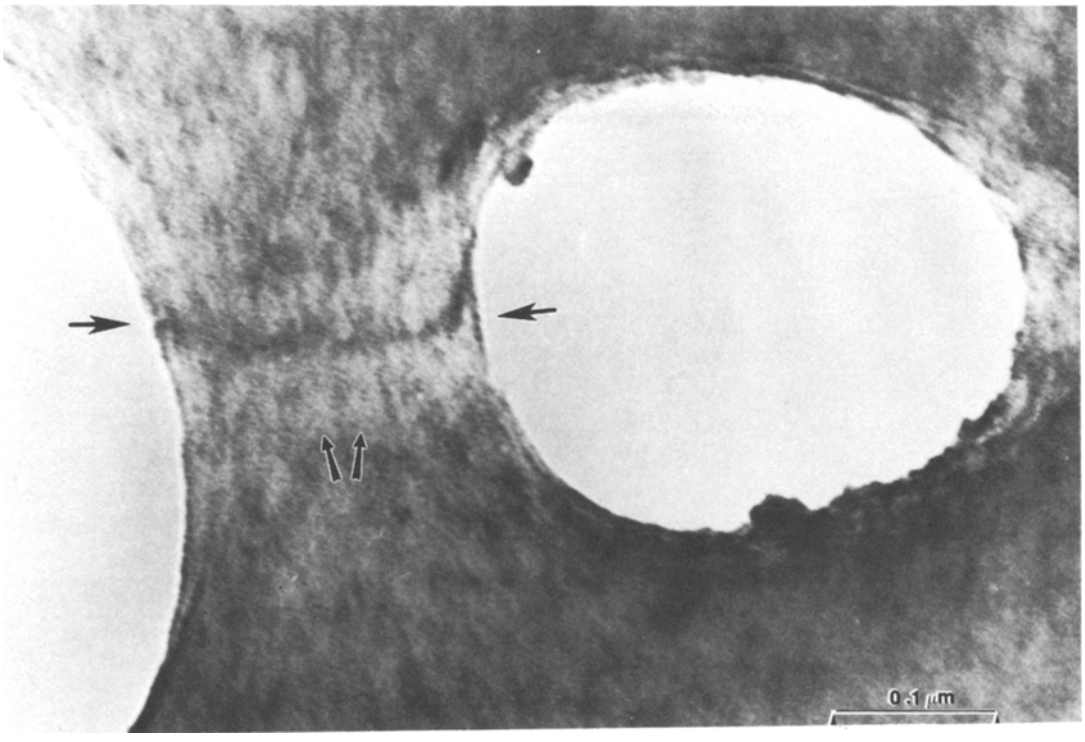

Figure 14 Heterogeneities in a standard-cure stoichiometric sample around a propagating crack.

may be seen that the post-cure temperature (175° C) is higher than the sample T_g in all cases.

A phenomenological explanation of the results presented is given below. In the studies of Yamini and Young [11], the samples were post-cured at room temperature for 24 h. Very limited reaction would have occurred in the samples at this stage. When the samples were post-cured at a higher temperature, a large number of nuclei will form at sites that are still unreacted, and the higher the post-curing temperature, the larger the number of nuclei [27]. Also curing will be more rapid at higher temperature. Thus the heterogeneity size would be expected to decrease with increase in post-curing temperature, as was observed by the authors. Aspbury and Wake [2], on the other hand, first cured the samples at 60° C for 4 days followed by a post-cure at 150° C for 8 h and observed that the heterogeneity size had almost doubled on post-curing. The results in the present investigation followed a cure cycle of 75° C for 2 h/125° C for 2 h followed by post-curing of 175° C for 6 h. The heterogeneity sizes in the five samples studied increased from 23–45 nm to 68–85 nm on post-curing. In these samples and also in the samples of Aspbury and Wake [2], considerable reaction had apparently already occurred in the initially cured samples themselves. Thus on post-curing, though the samples are in a rubber-like state, the number of available unreacted sites will be limited. Thus the new entities will form as a result of reorganization of the pre-existing heterogeneous morphology of this sample rather than by the formation and growth of new nuclei.

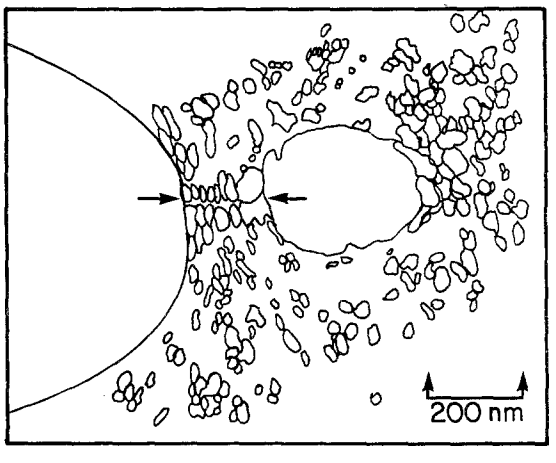

Figure 15 The deformation and alignment of the heterogeneities around the propagating crack.

However, since the mechanism of reorganization has not been studied, no comments on this aspect can be offered at this stage.

5. Conclusions

A combination of techniques of sample preparation and of sample examination show that the cured epoxy resin system investigated has a heterogeneous morphology and that the sizes of the spherical entities obtained from these different methods are reasonably consistent. The heterogeneities are entities of higher crosslink density in a matrix of relatively lower crosslink density. The fracture path is around the heterogeneity and not through it. Rapid curing results in small heterogeneities in the stoichiometric sample. In other samples containing an excess of epoxy or amine, relatively slower curing apparently results in larger heterogeneities. The increase in heterogeneity size on post-curing has been attributed to reorganization of the pre-existing entities.

Acknowledgements

The authors are grateful to Dr Y. L. Chen and Mr R. Bacon for assistance with the SEM, Ms P. Lloyd for microtomy, Mr Dolf Biermann for plasma-etching, Ms Mary K. Hershey for the Fourier transform infrared osmium tetroxide reactivity study, Dr S. Kumar for size measurement studies, and Natalie Sevy for typing of the manuscript. One of the authors (V. B. Gupta) is grateful to the Air Force Systems Command and the National Research Council, Washington, DC, for the award of an Associateship during 1982–84 and to the Indian Institute of Technology, New Delhi, for the grant of leave.

References

1. A. OBERLIN, J. AYACHE, M. OBERLIN and M. GUIGON, *J. Polym. Sci., Polym. Phys. Ed.* **20** (1982) 579.
2. P. J. ASPBURY and W. C. WAKE, *Brit. Polym. J.* **11** (1979) 17.
3. J. L. RACICH and J. A. KOUTSKY, "Chemistry and Properties of Crosslinked Polymers", edited by S. S. Labana (Academic Press, New York, 1977).
4. *Idem., J. Appl. Polym. Sci.* **20** (1976) 2111.
5. J. MIJOVIC and J. A. KOUTSKY, *Polymer* **20** (1979) 1095.
6. J. A. MANSON, L. H. SPERLING and S. L. KIM, "Influence of Crosslinking on the Mechanical Properties of High T_g Polymers", Technical Report AFML-TR-77-109 (July 1977).
7. S. C. MISRA, J. A. MANSON and L. H. SPERLING, "Epoxy Resin Chemistry", edited by R. S. Bauer, ACS Symp. Ser. 114 (American Chemical Society, Washington, DC, 1979) p. 157.
8. J. P. BELL, *J. Appl. Polym. Sci.* **27** (1982) 3503.
9. T. TAKAHAMA and P. H. GEIL, *Makromol. Chem., Rapid Commun.* **3** (1982) 389.
10. R. J. MORGAN and J. E. O'NEAL, *J. Mater. Sci.* **12** (1977) 1966.
11. S. YAMINI and R. J. YOUNG, *ibid.* **15** (1980) 1823.
12. I. M. BROWN and T. C. SANDRECZKI, *Polym. Preprints* **23** (1982) 199.
13. I. M. BROWN, A. C. LIND and T. C. SANDRECZKI, "Magnetic Resonance Studies of Epoxy Resins", McDonnell Douglas Research Labs, St Louis, Missouri, Report No. MDCQ 0721.
14. R. J. MATYI, D. P. UHLMANN and J. A. KOUTSKY, *J. Polym. Sci., Polym. Phys. Ed.* **18** (1980) 1053.
15. V. T. KREIBICH and R. SCHMID, *J. Polym. Sci. Symp.* **53** (1975) 177.
16. E. S. W. KONG, *Compos. Technol. Rev.* **4** (1982) 97.
17. W. FUNKE, *Chimia* **22** (1968) 111.
18. W. FUNKE, W. BEER and V. SEITZ, *Progr. Colloid Polym. Sci.* **57** (1975) 48.
19. S. S. LABANA, S. NEWMAN and A. J. CHOMPFF, "Polymer Networks", edited by A. J. Chompff and S. Newman (Plenum Press, New York, 1971) p. 453.
20. S. LUNAK and K. DUSEK, *J. Polym. Sci. Symp.* **53** (1975) 45.
21. K. DUSEK, J. PLESTIL, F. LEDNICKY and S. LUNAK, *Polymer* **19** (1978) 393.
22. R. D. DEANIN, Polymer Structure, Properties, and Applications" (Cahners, Boston, Mass., 1972) p. 354.
23. E. G. BOBALEK, E. R. MOORE, S. S. LEVY and C. C. LEE, *J. Appl. Polym. Sci.* **11** (1967) 1593.
24. D. H. SOLOMON, *J. Macromol. Sci. Rev.* **C-1** (1) (1967) 179.
25. A. APICELLA, L. NICOLAIS and J. C. HALPIN, 28th National SAMPE Symposium on Materials and Processes – Continuing Innovations, April 1983 (SAMPE, Covina, CA, 1983) p. 518.
26. G. C. STEVENS, J. V. CHAMPION and P. LIDDELL, *J. Polym. Sci. Polym. Phys. Ed.* **20** (1982) 327
27. K. E. LUTTGERT and R. BONART, *Prog. Colloid Polym. Sci.* **64** (1978) 38.
28. M. D. SKIBO, R. W. HERTZBERG and J. A. MANSON, *J. Mater. Sci.* **11** (1976) 479.
29. V. B. GUPTA, L. T. DRZAL and R. OMLOR, Procedings of 41st Annual Meeting of the Electron Miscroscopy Society of America, edited by G. W. Bailey (San Francisco Press, San Francisco, 1983) p. 36.
30. V. B. GUPTA, L. T. DRZAL, C. Y-C. LEE and M. J. RICH, *J. Macromol. Sci. Phys.* in press.
31. R. N. HAWARD and I. BROUGH, *Polymer* **10** (1969) 724.

Received 5 July
and accepted 20 September 1984